



Article

Monitoring the Conformational Changes of the A β (25–35) Peptide in SDS Micelles: A Matter of Time

Angelo Santoro ^{1,2,†} , Michela Buonocore ^{1,3,†} , Manuela Grimaldi ¹ , Enza Napolitano ^{1,4}
and Anna Maria D'Ursi ^{1,*}

- ¹ Department of Pharmacy, University of Salerno, Via Giovanni Paolo II, 132, 84084 Fisciano, Italy
² Department of Pharmacy, Scuola di Specializzazione in Farmacia Ospedaliera, University of Salerno, Via Giovanni Paolo II, 132, 84084 Fisciano, Italy
³ Department of Veterinary Pathology, University of Naples Federico II, Via Federico Delpino 1, 80137 Naples, Italy
⁴ PhD Program in Drug Discovery and Development, Department of Pharmacy, University of Salerno, 84084 Fisciano, Italy
* Correspondence: dursi@unisa.it
† These authors contributed equally to this work.

Abstract: Alzheimer's disease is a neurodegenerative disease characterized by the formation of amyloid plaques constituted prevalently by amyloid peptides. Due to the well-known challenges related to the study in solution of these peptides, several membrane-mimicking systems such as micelle constituted by detergent—i.e., DPC and SDS—have been deeply investigated. Additionally, the strategy of studying short fragments instead of the full-length peptide turned out to be advantageous in exploring the structural properties of the different moieties in A β in order to reproduce its pathologic effects. Several studies reveal that among A β fragments, A β (25–35) is the shortest fragment able to reproduce the aggregation process. To enrich the structural data currently available, in the present work we decided to evaluate the conformational changes adopted by A β (25–35) in SDS combining CD and NMR spectroscopies at different times. From the solved structures, it emerges that A β (25–35) passes from an unordered conformation at the time of the constitution of the system to a more ordered and energetically favorable secondary structure at day 7, which is kept for 2 weeks. These preliminary data suggest that a relatively long time affects the kinetic in the aggregation process of A β (25–35) in a micellar system, favoring the stabilization and the formation of a soluble helix conformation.

Keywords: Alzheimer; A β (25–35); NMR; structural biology; micelles



Citation: Santoro, A.; Buonocore, M.; Grimaldi, M.; Napolitano, E.; D'Ursi, A.M. Monitoring the Conformational Changes of the A β (25–35) Peptide in SDS Micelles: A Matter of Time. *Int. J. Mol. Sci.* **2023**, *24*, 971. <https://doi.org/10.3390/ijms24020971>

Academic Editors: Kenjiro Ono, Masashi Tanaka and Satoshi Saito

Received: 3 December 2022
Revised: 28 December 2022
Accepted: 31 December 2022
Published: 4 January 2023



Copyright: © 2023 by the authors. Licensee MDPI, Basel, Switzerland. This article is an open access article distributed under the terms and conditions of the Creative Commons Attribution (CC BY) license (<https://creativecommons.org/licenses/by/4.0/>).

1. Introduction

Alzheimer's disease (AD) is a neurodegenerative disease responsible for the slow and progressive destruction of brain cells, a condition which promotes the onset of total mental decline [1–3]. Nowadays, over 50 million people are affected by Alzheimer's or related dementia [4]. Based on the amyloid cascade hypothesis, the neurodegeneration caused by AD is due to the formation of fibrils composed of aggregated amyloid peptides and consequent plaques [5–9]. It is known that the aggregation process of amyloid- β (A β) peptides may be influenced by different factors, like metal ions, pH, temperature, and the environment in which they are located [10–12]. Several studies based on solid-state nuclear magnetic resonance (ssNMR) demonstrated that the full-length A β (1–40) and A β (1–42) tend to form polymorphic protofibrils which rearrange as raw β -sheet structures, predictive of β -organized superstructures in mature fibrils. However, the intermediate states leading to protofibrils are still under investigation [13–15]. Moreover, the rapid aggregation mechanism of these peptides raises an issue in setting the in vivo conditions

to study A β peptides in solution because a barely aqueous system would drive the self-interaction between the highly hydrophobic C-terminal region and the central A β moiety, forming the transient β -hairpin crucial for the aggregation process [9,16].

Although A β peptides tend to fibrillate in plain water, the interaction with the cell membrane is believed to be crucial for the pathological role of the peptide [17]. Therefore, several membrane-mimicking systems have been explored to study A β and its fragments. Mixtures of organic solvents—such as trifluoroethanol (TFE) and 1,1,1,3,3,3-hexafluoro-2-propanol (HFIP)—with water were largely exploited mainly in early structural studies of A β peptides [18–26]. Micelles, on the other hand, represent one of the most used membrane-mimetic systems thanks to their low molecular weight and high reproducibility. In a recent study, Serra-Batiste et al. explored various surfactant micelles for the formation of oligomeric complexes. They demonstrated that in dodecyl phosphocholine (DPC) micelles A β (1–42) peptide, rather than A β (1–40), β -sheet-structured oligomers tends to form due to the higher hydrophobic nature of the longer amyloid- β fragment [27,28]. Another membrane-mimetic system extensively used for studying A β peptides is sodium dodecyl sulphate (SDS) micelles. Indeed, A β peptides are characterized by an overall positive charge, which allows the peptides to interact with the negatively charged surface formed by SDS micelles [21,29]. Conformational studies of wild-type and mutant A β peptides in SDS demonstrated that the peptide–micelles interaction is significantly affected by the primary structure [30–32]. Still, obtaining the full-length amyloid peptides is not a simple task, and several works have focused their study on shorter domains of A β peptide, which are excellent starting points for probing the behavior of parent proteins in different systems [24,33–37]. Several A β fragments react similarly to the parent peptides when placed in the SDS micelle system. In particular, different studies have been performed to investigate the behavior in SDS micelles of A β fragments encompassing residues $^{10}\text{Y-M}^{35}$ [38–41]. Among these fragments, A β (25–35) represents the shortest sequence of A β able to mimic the biological behavior of the full-length amyloid peptides, forming large β -sheet aggregates and reproducing the toxicity of the peptide [21,42–45]. Conformational studies indicate that A β (25–35), like A β (1–42), undergoes a conformational transition depending on the environmental conditions, passing from a soluble and unordered secondary structure to an aggregated fibrillary β -sheet structure [46]. Previous conformational analysis of A β (25–35), performed with nuclear magnetic resonance (NMR) in SDS and LiDS micelle solutions, demonstrated the presence of a helix on $^{28}\text{K-L}^{34}$, proving that A β (25–35) has structural features similar to its parent peptide A β (1–42) [47]. As the amyloid peptide tends to aggregate over time, the great threat is represented by the final formation of the pathological amyloid plaques [48–50]. Because this often represents a point of no return, it is fundamental to mitigate and, in the most promising hypothesis, reverse this process while in the prodrome stages of the pathology. Although it is assessed that the setting of the environment is crucial to modulate the conformational events that bring to the formation of the fibrils, little is known about how time would gradually affect the secondary structure of amyloid in solution. In this work, we exploited A β (25–35) as a model to mimic the structural features of the A β (1–42) full-length, in the folding–unfolding process, with careful attention to the conformational intermediates occurring during the soluble-aggregate transition. To this end, we performed circular dichroism (CD) and NMR analysis to evaluate the effect of SDS micelles on the conformation of A β (25–35) at days 0, 4, 7, and 14; additionally, we measured the diffusion coefficients and the hydrodynamic radii of A β (25–35) at different times to investigate the behavior of the peptide–micelle complex.

2. Results

2.1. Circular Dichroism Experiments

Figure 1 shows CD spectra of A β (25–35) recorded in SDS micelle solution at the time of the constitution of the system and after 4, 7, and 14 days. The CONTIN analysis indicates that A β (25–35) in SDS micelles at day 0 presents 52% of random coil and 39% of β -sheet

conformation. After 4 days the content of β -sheet is unchanged, but there is an increase in the helix conformation (35–40%) at expenses of the random coil conformation. The increased ratio in helix conformation is conserved for the full duration of the experiments.

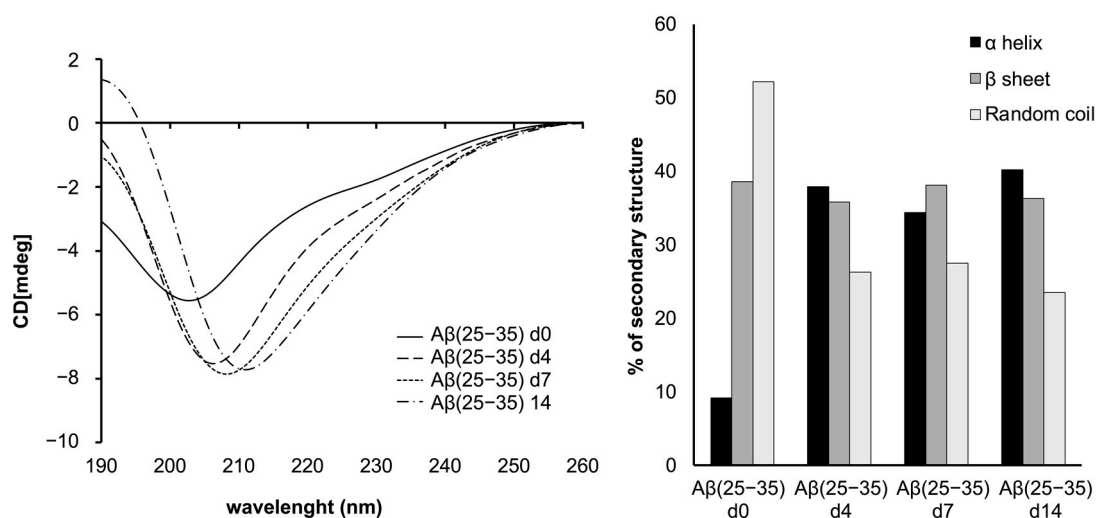


Figure 1. CD curves and secondary structure quantification performed with CONTIN algorithm of A β (25–35) peptide in SDS micelles at the time of the constitution of the system and after 4, 7 and 14 days.

2.2. NMR Spectroscopy

2.2.1. DOSY Experiments

To analyze the diffusion behavior of A β (25–35) peptide in the SDS micelle solution over time, we recorded pseudo-2D DOSY experiments. Details about DOSY spectra and diffusion curves are reported in Figures S1 and S2. Table 1 shows the diffusion coefficients of SDS micelles and A β (25–35) peptide, respectively.

Table 1. Diffusion (D) values (m^2/s) of A β (25–35) in SDS obtained by DOSY experiments.

| | D (m^2/s) SDS | D (m^2/s) A β (25–35) |
|--------|---------------------------------|---|
| Day 0 | $6.98 \pm 0.06 \times 10^{-11}$ | $6.78 \pm 0.07 \times 10^{-11}$ |
| Day 4 | $6.67 \pm 0.40 \times 10^{-11}$ | $6.45 \pm 0.17 \times 10^{-11}$ |
| Day 7 | $6.45 \pm 0.04 \times 10^{-11}$ | $6.43 \pm 0.19 \times 10^{-11}$ |
| Day 14 | $6.58 \pm 0.19 \times 10^{-11}$ | $6.60 \pm 0.14 \times 10^{-11}$ |

The diffusion coefficients (D) calculated from DOSY spectra for SDS micelles and A β (25–35) at different time points are very similar. The calculation of the hydrodynamic radius are based on the diffusion coefficient of A β (25–35) and SDS detergent, respectively, using 1,4-dioxane as a reference resulted in a 26 Å hydrodynamic radius [51]. This value corresponds to the R_h calculated for SDS micelles in water [52–54]. It is constant for all the experimental conditions, and as is common to SDS and A β (25–35) peptide, indicates an interaction of the peptide with the SDS micelles which is conserved over time.

2.2.2. Analysis of A β (25–35) Structures

1D ^1H , 2D ^1H - ^1H Total Correlation Spectroscopy (TOCSY) and Nuclear Overhauser Effect Spectroscopy (NOESY) spectra of A β (25–35) in SDS micelles at 0, 4, 7 and 14 days were collected on a Bruker 600 MHz at 298 K (Figures S3–S6). A ^1H chemical shift assignment was carried out by iteratively analyzing TOCSY and NOESY spectra with SPARKY [55,56]. 2D ^1H - ^1H spectra show 11 well-dispersed amide chemical shifts and uniform resonance line

widths according to the characteristics of a structured peptide (Tables S1–S4). The sequential chemical shift assignment was performed according to the Wüthrich procedure [57]. The NOEs were translated into interprotonic distances using CALIBA routine of CYANA 3.1 software and then used as restraints for the NMR structure calculations [58]. Table 2 reports the statistics for the structural calculation of the NMR ensemble of A β (25–35) peptide at 0, 4, 7, and 14 days in SDS micelles. The table shows a significant increase in total NOEs recorded in the different NOESY spectra over time.

Table 2. Statistics for the structural calculation of the NMR ensemble of A β (25–35) peptide at 0, 4, 7, and 14 days in SDS micelles.

| | Day 0 | Day 4 | Day 7 | Day 14 |
|---|-----------|-----------|-----------|-----------|
| Number of Experimental Restraints after CYANA | | | | |
| Total NOEs | 169 | 203 | 217 | 217 |
| Intra residual | 112 | 118 | 123 | 121 |
| Short-range | 53 | 56 | 60 | 60 |
| Medium-range | 4 | 29 | 34 | 36 |
| Long-range | 0 | 0 | 0 | 0 |
| RMSD | | | | |
| bb/heavy Å | 2.15/3.09 | 0.63/1.21 | 0.58/1.21 | 0.25/0.94 |
| Ramachandran analysis | | | | |
| Favorable regions | 40.0% | 40.6% | 41.7% | 84.3% |
| Additional allowed regions | 41.7% | 43.1% | 29.7% | 14.3% |
| Generously allowed regions | 18.0% | 14.9% | 28.6% | 1.1% |
| Disallowed regions | 0.3% | 1.4% | 0.0% | 0.3% |

Figure 2 summarizes the sequential and medium-range NOE effects observed in the 2D NOESY spectra. The sequential NOE plots report at day 0 only one α ,N(i,i+2) effect between residues ^{29}G - G^{33} . The paucity of NOE reveals the prevalence of disordered conformations with the presence of rare half-turn structures in the central part of the peptide. From day 4, several N,N(i,i+2), α ,N(i,i+2), α ,N(i,i+3) and α , β (i,i+3) effects indicate the rising of turn-helical structures involving the residues ^{29}G - M^{35} . On days 7–14, additional NOEs are observable in the N-terminal region, consistent with the rising of stable, regular secondary structures including all the peptide sequence. Interestingly, analysis of the NMR structure bundle indicates a progressive reduction of the conformer families moving from day 0 to day 14. At the beginning, A β (25–35) is disordered: a variety of conformer populations are evident, with a sporadic half-turn on the N-terminus. From day 4, high occurrence of regular conformations is evident, with the definition of a 3_{10} helix on the residues ^{28}K - I^{32} at day 14.

The Ramachandran plots in Figure 3 confirm that A β (25–35) at day 0 is characterized by three different clusters of conformations, which are β -sheet, right-handed and left-handed helix. Starting from day 4, the peptide loses the contribution provided by the β -sheet secondary structure, still conserving both orientations of the helix conformation. Conversely, at days 7 and 14, the peptide assumes predominantly right-handed helix conformation.

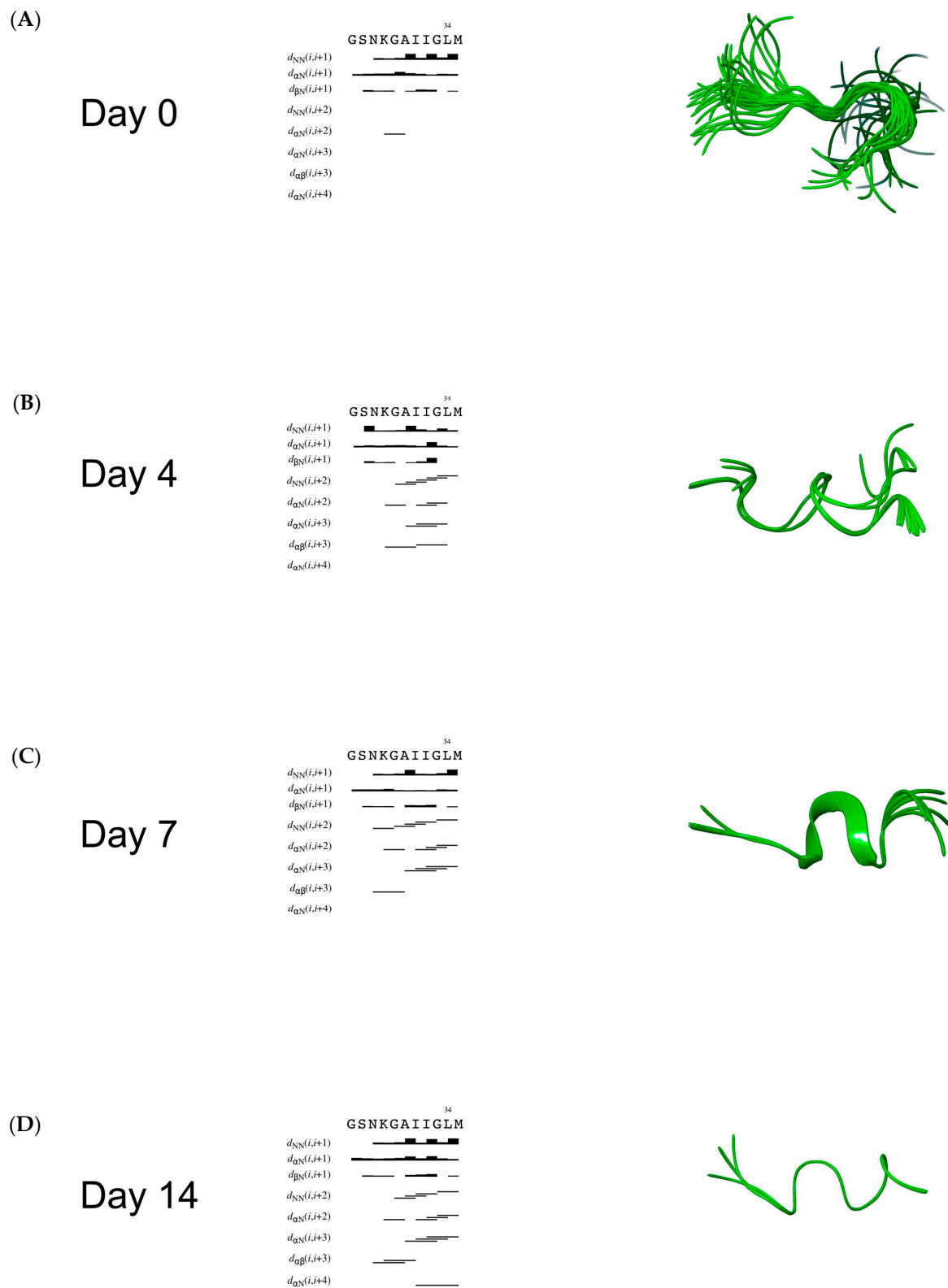


Figure 2. On the left, overview of the sequential and medium-range nuclear Overhauser enhancements (NOEs) used to calculate the A β (25–35) structure ensembles obtained at day 0 (A), day 4 (B), day 7 (C) and day 14 (D). On the right, ribbon visualization of the representative structures of the corresponding calculated ensembles.

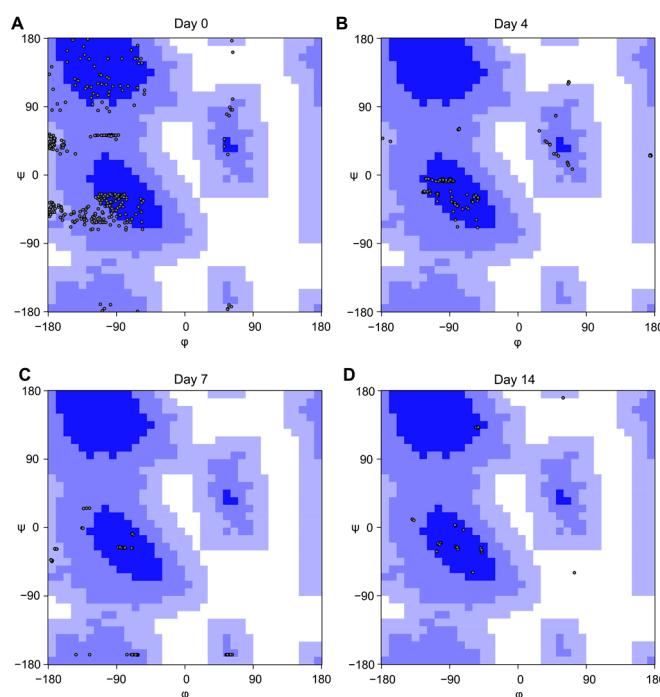


Figure 3. Ramachandran plot of A β (25–35) peptide at (A) day 0, (B) day 4, (C) day 7, and (D) day 14 in SDS micelles.

Procheck-NMR analysis performed on the solved A β (25–35) PDB structures [59] allowed obtaining the Ramachandran plot for each residue of the NMR-calculated bundle of structures. Based on this analysis, we observed that A β (25–35) N-terminal and C-terminal residues tend to assume over time dihedral angle values close to those of a right-handed helix (Figure S9A–D). By comparing these values with those deposited in PDB for A β (1–40) NMR structure in SDS (PDB ID: 1BA4) (Figure S9E), it is possible to affirm that the structure of the short A β (25–35) after 14 days is similar to the A β (1–40)'s, validating the use of A β (25–35) as a valuable A β (1–40) structural model [29].

3. Discussion

Aggregation of A β peptide is a matter of time and modulating the formation of the monomers or the soluble fibrils could represent a winning strategy to prevent AD [60]. Unfortunately, this is a very difficult task because of the tendency of amyloid peptides to aggregate in aqueous conditions, which makes these molecules troublesome to study in an experimental context. In this regard, systems of micelles composed of SDS have been exploited to study the solution structures for the full-length A β (1–42) and several fragments [27,28,30,31,61], among which, A β (25–35) represents the shortest portion capable of mimicking the aggregation process [21,24,42,45,47]. In this work, we study the behavior of A β (25–35) in SDS at 0, 4, 7, and 14 days to gain insights on the conditions in which this fragment can reproduce to the greatest extent the features of the full-length in this system. Preliminary CD analysis shows that A β (25–35) in SDS passes from a tendentially disordered conformation at day 0, characterized by prevalent random coil and β -sheet conformations, to a more ordered one, after four days, where the helix conformations rise and increase for over the experimented time (Figure 1). Diffusion experiments performed by NMR spectroscopy evidence that the peptide A β (25–35) interacts with the micelles right from the early stages, suggesting a behavior comparable with other amyloid peptide fragments, whose interaction with SDS micelles has been widely studied [41,61]. This interaction is maintained throughout the analysis as confirmed by the diffusion values and the hydrodynamic radii similar to SDS micelles' ones, in accordance with data reported in literature [62–64]. Two-dimensional TOCSY and NOESY experiments revealed that NOE

effects between the peptide's protons significantly increase from day 0 to day 4, particularly in the $^{28}\text{K-M}^{35}$ region. Indeed, at days 7–14, this effect is also extended to residue ^{27}N , suggesting that the peptide tends to stabilize its conformation over time. The transition to ordered conformations is evident in the 2D-NOESY spectra with the appearance of new inter-residues peaks. $\text{A}\beta(25-35)$ in SDS passes from unstable β -like conformation to a more ordered and stable α -helix structure encompassing the residues $^{29}\text{G-M}^{35}$ after 7 days (Figure 2). Eventually, at day 14, this α -helix conformation converts to a 3_{10} helix and shifts on the residues $^{28}\text{K-I}^{32}$. These data suggest that the C-terminus represents the $\text{A}\beta(25-35)$ moiety most affected by the effects of the time in the proposed system. The Ramachandran plot analysis supports this evidence: at day 0 $\text{A}\beta(25-35)$ presents a structure with a dense cluster of dihedral angles in the β -sheet region (Figure 3A), which is already lost at day 4 (Figure 3B) in favor of a rather helical structure, whereas at days 7 and 14 there is a lower number of clusters, all concentrated in the region of right-handed helix dihedral angle values (Figure 3C,D). By analyzing the Ramachandran plot residue by residue, it is possible to observe that the residues primarily involved in the β -sheet conformation are situated in the N-terminus (Figure S9A). However, it is possible to observe that for all the residues of the sequence the dihedral angle values tend to cluster at day 7 in helix conformations, except for the $^{33}\text{G-L}^{34}$ amino acids which are characterized by regular helix structures only at day 14. Remarkably, by comparing the $\text{A}\beta(25-35)$ dihedral angle values obtained on the last day with those of the corresponding residues of $\text{A}\beta(1-40)$ in SDS (PDB ID: 1BA4), it is possible to observe a significant similarity of the structures (Figure S9D,E). In conclusion, this explorative study highlights that the amyloid fragment may prefer a 7-day delay of settling from the time of the constitution of the system to assume energetically favorable conformations, similar to those of the parent $\text{A}\beta(1-40)$ amyloid peptide in the same conditions. Therefore, it is mandatory that special attention be given to the choice of timing when negatively charged micelles are chosen for structural studies.

4. Materials and Methods

4.1. Sample Preparation

4.1.1. $\text{A}\beta(25-35)$ Peptide Synthesis

$\text{A}\beta(25-35)$, was manually synthesized using Fmoc/tBu solid-phase peptide synthesis (SPPS) following Merrifield strategy [37,65]. The peptide was purified by reversed-phase chromatography (HPLC) using Phenomenex C18 column. The peptides were characterized on a Finnigan LCQ Deca ion trap instrument equipped with an electrospray source (LCQ Deca Finnigan, San José, CA, USA). The samples were directly infused in the ESI source using a syringe pump at a flow rate of 5.0 mL/min. The data were analyzed using the Xcalibur software. The sample purity was >98%.

4.1.2. Sample Preparation for Analyses

Before performing experiments, $\text{A}\beta(25-35)$ peptide was previously treated according to the defibrillation procedure [66]. Subsequently, SDS micelles were prepared by dissolving $\text{A}\beta(25-35)$ peptide in an SDS/PBS (pH 7.4) mixture. To obtain SDS micelles, we used a concentration of 80 mM, which is 10-fold the SDS critical micellar concentration (c.m.c.) [67]. The final concentration of $\text{A}\beta(25-35)$ peptide was 0.15 mM.

4.2. CD Experiments

CD spectra were obtained using a JASCO J-810 spectropolarimeter, with the aid of a 1 mm long quartz cell, working at a temperature of 25 °C. The CD curves were acquired by an average of 4 scans, in a measuring range of 260–190 nm, at a bandwidth of 1 nm and at a scanning speed of 10 nm/min. Each spectrum was processed by subtracting the solvent spectrum. The analysis of the CD curves was performed using the CONTIN algorithm of the online platform DICHROWEB [68,69].

4.3. NMR Experiments

4.3.1. NMR Data Recording and Processing

A β (25–35) and SDS-d₂₅ were prepared as described before. All NMR samples were given 10% (v/v) D₂O. Further, 1D, 2D (¹H-¹H-TOCSY and ¹H-¹H-NOESY), and pseudo-2D (DOSY) experiments were recorded at 25 °C on a Bruker Avance 600 MHz spectrometer equipped with a 5 mm triple resonance ¹H, ¹³C and ¹⁵N, z-axis pulsed-field gradient probe head. The water signal was suppressed using the excitation sculpting gradient pulse [70]. All the spectra were transformed and visualized in TopSpin 3.1 (Bruker Biospin). For the structure calculation of A β (25–35) peptide at different time, 2D spectra were iteratively analyzed using SPARKY software [55,56]. Chemical shifts assignment was obtained using the standard approach described by Wuthrich [57]. Diffusion constants of peptide over time were acquired by pseudo 2D diffusion ordered spectroscopy (DOSY) experiments by a stimulated echo bipolar pulse field gradient (stebpgp1s) program [71,72]. A total of 32 spectra with gradient strengths ranging from 2% to 98% of the maximum value were recorded. A diffusion time Δ of 60 ms and gradient length δ of 1.0 ms were used in all the experiments. The spectra were analyzed using TopSpin Dynamics Center (Bruker, Fällanden, Switzerland). The diffusion values were obtained by fitting the peak intensity decays using the Stejskal-Tanner equation [73]:

$$f(g) = I_0 e^{-\gamma^2 g^2 \delta^2 (\Delta - \frac{\delta}{3}) D}$$

Using the Wilkins equation, it was possible to determine the hydrodynamic radius (R_h) of A β (25–35) peptide from the diffusion values. We added 1,4-dioxane to a final concentration of 10 mM as internal standard. Because the hydrodynamic radius value of 1,4-dioxane is tabulated as 2.12 Å, it was used as an internal reference and used for the calculation of R_h [51,74]:

$$R_{h,prot} = \frac{D_{ref} \cdot R_{h,ref}}{D_{prot}}$$

where D_{ref} and $R_{h,ref}$, respectively, are the diffusion and the hydrodynamic radius of the internal reference, and D_{prot} and $R_{h,prot}$, respectively, are the diffusion and the hydrodynamic radius of A β (25–35) peptide.

4.3.2. Structure Calculations

NOESY peaks were integrated using the Gaussian fit integration method of SPARKY software. Peak volumes deriving from the assignment were translated into upper distance bounds with the CALIBA routine from the CYANA 2.1 software package [58]. Redundant and duplicate constraints were discarded for each sample, and the final list of constraints was used to generate a set of 50 structures using the CYANA protocol of simulated annealing in torsion angle space (50000 steps). Entries presenting the lowest target function value (2–12) and irrelevant residual violation (maximum violation 0.71 Å) were analyzed using Schrodinger's Maestro 12.5.139 [75]. Procheck-NMR was used to assess the quality of the structures and to analyze the dihedral angles [59].

Supplementary Materials: The following supporting information can be downloaded at: <https://www.mdpi.com/article/10.3390/ijms24020971/s1>.

Author Contributions: Conceptualization, A.M.D.; software, A.S. and M.B.; validation, A.S. and M.B.; formal analysis, A.S., M.B., M.G. and E.N.; investigation, A.S. and M.B.; resources, A.M.D.; data curation, A.S., M.B., M.G. and E.N.; writing—original draft preparation, A.S. and M.B.; writing—review and editing, A.M.D.; visualization, A.M.D.; supervision, A.M.D.; project administration, A.M.D.; funding acquisition, A.M.D. All authors have read and agreed to the published version of the manuscript.

Funding: This research received no external funding.

Institutional Review Board Statement: Not applicable.

Informed Consent Statement: Not applicable.

Data Availability Statement: Not applicable.

Conflicts of Interest: The authors declare no conflict of interest.

References

1. Prince, M.; Bryce, R.; Albanese, E.; Wimo, A.; Ribeiro, W.; Ferri, C.P. The global prevalence of dementia: A systematic review and metaanalysis. *Alzheimer's Dement.* **2013**, *9*, 63–75.e2. [[CrossRef](#)] [[PubMed](#)]
2. Fiandaca, M.S.; Mapstone, M.E.; Cheema, A.K.; Federoff, H.J. The critical need for defining preclinical biomarkers in Alzheimer's disease. *Alzheimer's Dement.* **2014**, *10*, S196–S212. [[CrossRef](#)] [[PubMed](#)]
3. Goyal, D.; Shuaib, S.; Mann, S.; Goyal, B. Rationally designed peptides and peptidomimetics as inhibitors of amyloid- β (A β) aggregation: Potential therapeutics of Alzheimer's disease. *ACS Comb. Sci.* **2017**, *19*, 55–80. [[CrossRef](#)] [[PubMed](#)]
4. Meyers, E.A.; Amouyel, P.; Bovenkamp, D.E.; Carrillo, M.C.; De Buchy, G.D.; Dumont, M.; Fillit, H.; Friedman, L.; Henderson-Begg, G.; Hort, J. Commentary: Global Alzheimer's disease and Alzheimer's disease related dementia research funding organizations support and engage the research community throughout the COVID-19 pandemic. *Alzheimer's Dement.* **2022**, *18*, 1067–1070. [[CrossRef](#)] [[PubMed](#)]
5. Hardy, J.A.; Higgins, G.A. Alzheimer's disease: The amyloid cascade hypothesis. *Science* **1992**, *256*, 184–185. [[CrossRef](#)]
6. Dickson, D.W. The pathogenesis of senile plaques. *J. Neuropathol. Exp. Neurol.* **1997**, *56*, 321–339. [[CrossRef](#)] [[PubMed](#)]
7. Selkoe, D.J. Translating cell biology into therapeutic advances in Alzheimer's disease. *Nature* **1999**, *399*, A23–A31. [[CrossRef](#)]
8. Hoyer, W.; Grönwall, C.; Jonsson, A.; Ståhl, S.; Härd, T. Stabilization of a β -hairpin in monomeric Alzheimer's amyloid- β peptide inhibits amyloid formation. *Proc. Natl. Acad. Sci. USA* **2008**, *105*, 5099–5104. [[CrossRef](#)]
9. Abelein, A.; Abrahams, J.P.; Danielsson, J.; Gräslund, A.; Jarvet, J.; Luo, J.; Tiiman, A.; Wärmländer, S.K. The hairpin conformation of the amyloid β peptide is an important structural motif along the aggregation pathway. *JBIC J. Biol. Inorg. Chem.* **2014**, *19*, 623–634. [[CrossRef](#)]
10. Ahmed, M.; Davis, J.; Aucoin, D.; Sato, T.; Ahuja, S.; Aimoto, S.; Elliott, J.I.; Van Nostrand, W.E.; Smith, S.O. Structural conversion of neurotoxic amyloid- β 1–42 oligomers to fibrils. *Nat. Struct. Mol. Biol.* **2010**, *17*, 561. [[CrossRef](#)]
11. Wärmländer, S.; Tiiman, A.; Abelein, A.; Luo, J.; Jarvet, J.; Söderberg, K.L.; Danielsson, J.; Gräslund, A. Biophysical Studies of the Amyloid β -Peptide: Interactions with Metal Ions and Small Molecules. *ChemBioChem* **2013**, *14*, 1692–1704. [[CrossRef](#)] [[PubMed](#)]
12. Wallin, C.; Luo, J.; Jarvet, J.; Wärmländer, S.K.; Gräslund, A. The Amyloid- β Peptide in Amyloid Formation Processes: Interactions with Blood Proteins and Naturally Occurring Metal Ions. *Isr. J. Chem.* **2017**, *57*, 674–685. [[CrossRef](#)]
13. Scheidt, H.A.; Morgado, I.; Rothmund, S.; Huster, D.; Fändrich, M. Solid-state NMR spectroscopic investigation of A β protofibrils: Implication of a β -sheet remodeling upon maturation into terminal amyloid fibrils. *Angew. Chem. Int. Ed.* **2011**, *50*, 2837–2840. [[CrossRef](#)]
14. Scheidt, H.A.; Morgado, I.; Rothmund, S.; Huster, D. Dynamics of amyloid β fibrils revealed by solid-state NMR. *J. Biol. Chem.* **2012**, *287*, 2017–2021. [[CrossRef](#)]
15. Scheidt, H.A.; Morgado, I.; Huster, D. Solid-state NMR reveals a close structural relationship between amyloid- β protofibrils and oligomers. *J. Biol. Chem.* **2012**, *287*, 22822–22826. [[CrossRef](#)] [[PubMed](#)]
16. Sandberg, A.; Luheshi, L.M.; Söllvander, S.; de Barros, T.P.; Macao, B.; Knowles, T.P.; Biverstål, H.; Lendel, C.; Ekholm-Petterson, F.; Dubnovitsky, A. Stabilization of neurotoxic Alzheimer amyloid- β oligomers by protein engineering. *Proc. Natl. Acad. Sci. USA* **2010**, *107*, 15595–15600. [[CrossRef](#)] [[PubMed](#)]
17. Kotler, S.A.; Walsh, P.; Brender, J.R.; Ramamoorthy, A. Differences between amyloid- β aggregation in solution and on the membrane: Insights into elucidation of the mechanistic details of Alzheimer's disease. *Chem. Soc. Rev.* **2014**, *43*, 6692–6700. [[CrossRef](#)] [[PubMed](#)]
18. Talafous, J.; Marcinowski, K.J.; Klopman, G.; Zagorski, M.G. Solution Structure of Residues 1–28 of the Amyloid. beta.-Peptide. *Biochemistry* **1994**, *33*, 7788–7796. [[CrossRef](#)] [[PubMed](#)]
19. Sticht, H.; Bayer, P.; Willbold, D.; Dames, S.; Hilbich, C.; Beyreuther, K.; Frank, R.W.; Rösch, P. Structure of amyloid A4-(1–40)-peptide of Alzheimer's disease. *Eur. J. Biochem.* **1995**, *233*, 293–298. [[CrossRef](#)] [[PubMed](#)]
20. Crescenzi, O.; Tomaselli, S.; Guerrini, R.; Salvadori, S.; D'Ursi, A.M.; Temussi, P.A.; Picone, D. Solution structure of the Alzheimer amyloid β -peptide (1–42) in an apolar microenvironment: Similarity with a virus fusion domain. *Eur. J. Biochem.* **2002**, *269*, 5642–5648. [[CrossRef](#)]
21. D'Ursi, A.M.; Armenante, M.R.; Guerrini, R.; Salvadori, S.; Sorrentino, G.; Picone, D. Solution structure of amyloid β -peptide (25–35) in different media. *J. Med. Chem.* **2004**, *47*, 4231–4238. [[CrossRef](#)] [[PubMed](#)]
22. Tomaselli, S.; Esposito, V.; Vangone, P.; van Nuland, N.A.; Bonvin, A.M.; Guerrini, R.; Tancredi, T.; Temussi, P.A.; Picone, D. The α -to- β conformational transition of Alzheimer's A β -(1–42) peptide in aqueous media is reversible: A step by step conformational analysis suggests the location of β conformation seeding. *ChemBioChem* **2006**, *7*, 257–267. [[CrossRef](#)] [[PubMed](#)]
23. Zirah, S.; Kozin, S.A.; Mazur, A.K.; Blond, A.; Cheminant, M.; Ségalas-Milazzo, I.; Debey, P.; Rebuffat, S. Structural changes of region 1–16 of the Alzheimer disease amyloid β -peptide upon zinc binding and in vitro aging. *J. Biol. Chem.* **2006**, *281*, 2151–2161. [[CrossRef](#)]

24. Österlund, N.; Luo, J.; Wärmländer, S.K.; Gräslund, A. Membrane-mimetic systems for biophysical studies of the amyloid- β peptide. *Biochim. Biophys. Acta-Proteins Proteom.* **2019**, *1867*, 492–501. [[CrossRef](#)] [[PubMed](#)]
25. Santoro, A.; Grimaldi, M.; Buonocore, M.; Stillitano, I.; D'Ursi, A.M. Exploring the early stages of the amyloid A β (1–42) peptide aggregation process: An NMR study. *Pharmaceuticals* **2021**, *14*, 732. [[CrossRef](#)]
26. Santoro, A.; Grimaldi, M.; Buonocore, M.; Stillitano, I.; Gloria, A.; Santin, M.; Bobba, F.; Saponetti, M.S.; Ciaglia, E.; D'Ursi, A.M. New A β (1–42) ligands from anti-amyloid antibodies: Design, synthesis, and structural interaction. *Eur. J. Med. Chem.* **2022**, *237*, 114400. [[CrossRef](#)] [[PubMed](#)]
27. Nadezhdin, K.; Bocharova, O.; Bocharov, E.; Arseniev, A. Structural and dynamic study of the transmembrane domain of the amyloid precursor protein. *Acta Nat.* **2011**, *3*, 69–76. [[CrossRef](#)]
28. Serra-Batiste, M.; Ninot-Pedrosa, M.; Bayoumi, M.; Gairí, M.; Maglia, G.; Carulla, N. A β 42 assembles into specific β -barrel pore-forming oligomers in membrane-mimicking environments. *Proc. Natl. Acad. Sci. USA* **2016**, *113*, 10866–10871. [[CrossRef](#)]
29. Coles, M.; Bicknell, W.; Watson, A.A.; Fairlie, D.P.; Craik, D.J. Solution structure of amyloid β -peptide (1–40) in a water–micelle environment. Is the membrane-spanning domain where we think it is? *Biochemistry* **1998**, *37*, 11064–11077. [[CrossRef](#)]
30. Shao, H.; Jao, S.C.; Ma, K.; Zagorski, M.G. Solution structures of micelle-bound amyloid β -(1–40) and β -(1–42) peptides of Alzheimer's disease. *J. Mol. Biol.* **1999**, *285*, 755–773. [[CrossRef](#)]
31. Rangachari, V.; Reed, D.K.; Moore, B.D.; Rosenberry, T.L. Secondary structure and interfacial aggregation of amyloid- β (1–40) on sodium dodecyl sulfate micelles. *Biochemistry* **2006**, *45*, 8639–8648. [[CrossRef](#)] [[PubMed](#)]
32. Usachev, K.S.; Filippov, A.; Khairutdinov, B.; Antzutkin, O.; Klochkov, V. NMR structure of the Arctic mutation of the Alzheimer's A β (1–40) peptide docked to SDS micelles. *J. Mol. Struct.* **2014**, *1076*, 518–523. [[CrossRef](#)]
33. Eichler, J. Peptides as protein binding site mimetics. *Curr. Opin. Chem. Biol.* **2008**, *12*, 707–713. [[CrossRef](#)] [[PubMed](#)]
34. Groß, A.; Hashimoto, C.; Sticht, H.; Eichler, J. Synthetic peptides as protein mimics. *Front. Bioeng. Biotechnol.* **2016**, *3*, 211. [[CrossRef](#)]
35. Marin, O.; Meggio, F.; Boldyreff, B.; Issinger, O.-G.; Pinna, L.A. Dissection of the dual function of the β -subunit of protein kinase CK2 ('casein kinase-2'): A synthetic peptide reproducing the carboxyl-terminal domain mimicks the positive but not the negative effects of the whole protein. *FEBS Lett.* **1995**, *363*, 111–114. [[CrossRef](#)]
36. Grimaldi, M.; Stillitano, I.; Amodio, G.; Santoro, A.; Buonocore, M.; Moltedo, O.; Remondelli, P.; D'Ursi, A.M. Structural basis of antiviral activity of peptides from MPER of FIV gp36. *PLoS ONE* **2018**, *13*, e0204042. [[CrossRef](#)]
37. Buonocore, M.; Santoro, A.; Grimaldi, M.; Covelli, V.; Firoznejhad, M.; Rodriguez, M.; Santin, M.; D'Ursi, A.M. Structural analysis of a simplified model reproducing SARS-CoV-2 S RBD/ACE2 binding site. *Heliyon* **2022**, *8*, e11568. [[CrossRef](#)]
38. Usachev, K.; Filippov, A.; Filippova, E.; Antzutkin, O.; Klochkov, V. Solution structures of Alzheimer's amyloid A β 13–23 peptide: NMR studies in solution and in SDS. *J. Mol. Struct.* **2013**, *1049*, 436–440. [[CrossRef](#)]
39. Rodziejewicz-Motowidło, S.; Czaplewska, P.; Sikorska, E.; Spodzieja, M.; Kołodziejczyk, A.S. The Arctic mutation alters helix length and type in the 11–28 β -amyloid peptide monomer—CD, NMR and MD studies in an SDS micelle. *J. Struct. Biol.* **2008**, *164*, 199–209. [[CrossRef](#)]
40. Usachev, K.S.; Filippov, A.V.; Antzutkin, O.N.; Klochkov, V.V. Use of a combination of the RDC method and NOESY NMR spectroscopy to determine the structure of Alzheimer's amyloid A β 10–35 peptide in solution and in SDS micelles. *Eur. Biophys. J.* **2013**, *42*, 803–810. [[CrossRef](#)]
41. Grimaldi, M.; Scrima, M.; Esposito, C.; Vitiello, G.; Ramunno, A.; Limongelli, V.; D'Errico, G.; Novellino, E.; D'Ursi, A.M. Membrane charge dependent states of the β -amyloid fragment A β (16–35) with differently charged micelle aggregates. *Biochim. Biophys. Acta (BBA)-Biomembr.* **2010**, *1798*, 660–671. [[CrossRef](#)] [[PubMed](#)]
42. Grimaldi, M.; Marino, S.D.; Florenzano, F.; Ciotta, M.T.; Nori, S.L.; Rodriguez, M.; Sorrentino, G.; D'Ursi, A.M.; Scrima, M. β -Amyloid-acetylcholine molecular interaction: New role of cholinergic mediators in anti-Alzheimer therapy? *Future Med. Chem.* **2016**, *8*, 1179–1189. [[CrossRef](#)] [[PubMed](#)]
43. Randino, R.; Grimaldi, M.; Persico, M.; De Santis, A.; Cini, E.; Cabri, W.; Riva, A.; D'Errico, G.; Fattorusso, C.; D'Ursi, A.M. Investigating the neuroprotective effects of turmeric extract: Structural interactions of β -amyloid peptide with single curcuminoids. *Sci. Rep.* **2016**, *6*, 38846. [[CrossRef](#)]
44. Sublimi Saponetti, M.; Grimaldi, M.; Scrima, M.; Albonetti, C.; Nori, S.L.; Cucolo, A.; Bobba, F.; D'Ursi, A.M. Aggregation of ass (25–35) on dopc and dopc/dha bilayers: An atomic force microscopy study. *PLoS ONE* **2014**, *9*, e115780. [[CrossRef](#)] [[PubMed](#)]
45. Pike, C.J.; Walencewicz-Wasserman, A.J.; Kosmoski, J.; Cribbs, D.H.; Glabe, C.G.; Cotman, C.W. Structure-activity analyses of β -amyloid peptides: Contributions of the β 25–35 region to aggregation and neurotoxicity. *J. Neurochem.* **1995**, *64*, 253–265. [[CrossRef](#)] [[PubMed](#)]
46. Terzi, E.; Hoelzelmann, G.; Seelig, J. Alzheimer. Beta-amyloid peptide 25–35: Electrostatic interactions with phospholipid membranes. *Biochemistry* **1994**, *33*, 7434–7441. [[CrossRef](#)]
47. Kohno, T.; Kobayashi, K.; Maeda, T.; Sato, K.; Takashima, A. Three-dimensional structures of the amyloid β peptide (25–35) in membrane-mimicking environment. *Biochemistry* **1996**, *35*, 16094–16104. [[CrossRef](#)] [[PubMed](#)]
48. Francis, F.; Koulakoff, A.; Boucher, D.; Chafey, P.; Schaar, B.; Vinet, M.-C.; Friocourt, G.; McDonnell, N.; Reiner, O.; Kahn, A. Doublecortin is a developmentally regulated, microtubule-associated protein expressed in migrating and differentiating neurons. *Neuron* **1999**, *23*, 247–256. [[CrossRef](#)] [[PubMed](#)]
49. Mattson, M.P. Pathways towards and away from Alzheimer's disease. *Nature* **2004**, *430*, 631–639. [[CrossRef](#)]

50. Aleksis, R.; Oleskovs, F.; Jaudzems, K.; Pahnke, J.; Biverstål, H. Structural studies of amyloid- β peptides: Unlocking the mechanism of aggregation and the associated toxicity. *Biochimie* **2017**, *140*, 176–192. [[CrossRef](#)]
51. Wilkins, D.K.; Grimshaw, S.B.; Receveur, V.; Dobson, C.M.; Jones, J.A.; Smith, L.J. Hydrodynamic radii of native and denatured proteins measured by pulse field gradient NMR techniques. *Biochemistry* **1999**, *38*, 16424–16431. [[CrossRef](#)] [[PubMed](#)]
52. Mazer, N.A.; Benedek, G.B.; Carey, M.C. An investigation of the micellar phase of sodium dodecyl sulfate in aqueous sodium chloride solutions using quasielastic light scattering spectroscopy. *J. Phys. Chem.* **1976**, *80*, 1075–1085. [[CrossRef](#)]
53. Shastry, T.A.; Morris-Cohen, A.J.; Weiss, E.A.; Hersam, M.C. Probing carbon nanotube–surfactant interactions with two-dimensional DOSY NMR. *J. Am. Chem. Soc.* **2013**, *135*, 6750–6753. [[CrossRef](#)]
54. Arkhipov, V.P.; Arkhipov, R.V.; Kuzina, N.A.; Filippov, A. Study of the premicellar state in aqueous solutions of sodium dodecyl sulfate by nuclear magnetic resonance diffusion. *Magn. Reson. Chem.* **2021**, *59*, 1126–1133. [[CrossRef](#)] [[PubMed](#)]
55. Goddard, T.; Kneller, D. *SPARKY 3.114*; University of California: San Francisco, CA, USA, 2007.
56. Kneller, D.; Kuntz, I. UCSF Sparky—an NMR display, annotation and assignment tool. *Proc. J. Cell. Biochem.* **1993**, *53*, 254.
57. Wüthrich, K. NMR with proteins and nucleic acids. *Eur. News* **1986**, *17*, 11–13. [[CrossRef](#)]
58. Güntert, P. Automated NMR structure calculation with CYANA. In *Protein NMR Techniques*; Springer: Berlin/Heidelberg, Germany, 2004; pp. 353–378.
59. Laskowski, R.A.; Rullmann, J.A.; MacArthur, M.W.; Kaptein, R.; Thornton, J.M. AQUA and PROCHECK-NMR: Programs for checking the quality of protein structures solved by NMR. *J. Biomol. NMR* **1996**, *8*, 477–486. [[CrossRef](#)] [[PubMed](#)]
60. Grover, S.; Jain, S. Aducanumab: A review of the first approved amyloid-targeting antibody for Alzheimer’s disease. *Drugs Ther. Perspect.* **2022**, *38*, 443–454. [[CrossRef](#)]
61. Marcinowski, K.J.; Shao, H.; Clancy, E.L.; Zagorski, M.G. Solution structure model of residues 1–28 of the Amyloid β -peptide when bound to micelles. *J. Am. Chem. Soc.* **1998**, *120*, 11082–11091. [[CrossRef](#)]
62. Thimons, K.L.; Brazdil, L.C.; Harrison, D.; Fisch, M.R. Effects of pentanol isomers on the growth of SDS micelles in 0.5 M NaCl. *J. Phys. Chem. B* **1997**, *101*, 11087–11091. [[CrossRef](#)]
63. Javadian, S.; Gharibi, H.; Sohrabi, B.; Bijanzadeh, H.; Safarpour, M.; Behjatmanesh-Ardakani, R. Determination of the physico-chemical parameters and aggregation number of surfactant in micelles in binary alcohol–water mixtures. *J. Mol. Liq.* **2008**, *137*, 74–79. [[CrossRef](#)]
64. Moore, P.N.; Puvvada, S.; Blankschein, D. Challenging the surfactant monomer skin penetration model: Penetration of sodium dodecyl sulfate micelles into the epidermis. *J. Cosmet. Sci.* **2003**, *54*, 29–46. [[PubMed](#)]
65. Merrifield, R.B. Solid-phase peptide synthesis. *Adv. Enzymol. Relat. Areas Mol. Biol.* **1969**, *32*, 221–296.
66. Jao, S.-C.; Ma, K.; Talafov, J.; Orlando, R.; Zagorski, M.G. Trifluoroacetic acid pretreatment reproducibly disaggregates the amyloid β -peptide. *Amyloid* **1997**, *4*, 240–252. [[CrossRef](#)]
67. Pellegrini, M.; Mierke, D.F. Structural characterization of peptide hormone/receptor interactions by NMR spectroscopy. *Pept. Sci.* **1999**, *51*, 208–220. [[CrossRef](#)]
68. Whitmore, L.; Wallace, B. DICHROWEB, an online server for protein secondary structure analyses from circular dichroism spectroscopic data. *Nucleic Acids Res.* **2004**, *32*, W668–W673. [[CrossRef](#)] [[PubMed](#)]
69. Whitmore, L.; Wallace, B.A. Protein secondary structure analyses from circular dichroism spectroscopy: Methods and reference databases. *Biopolym. Orig. Res. Biomol.* **2008**, *89*, 392–400. [[CrossRef](#)]
70. Parella, T.; Adell, P.; Sánchez-Ferrando, F.; Virgili, A. Effective multiple-solvent suppression scheme using the excitation sculpting principle. *Magn. Reson. Chem.* **1998**, *36*, 245–249. [[CrossRef](#)]
71. Stilbs, P. Molecular self-diffusion coefficients in Fourier transform nuclear magnetic resonance spectrometric analysis of complex mixtures. *Anal. Chem.* **1981**, *53*, 2135–2137. [[CrossRef](#)]
72. Vasenkov, S.; Galvosas, P.; Geier, O.; Nestle, N.; Stallmach, F.; Kärger, J. Determination of genuine diffusivities in heterogeneous media using stimulated echo pulsed field gradient NMR. *J. Magn. Reson.* **2001**, *149*, 228–233. [[CrossRef](#)]
73. Stejskal, E.O.; Tanner, J.E. Spin diffusion measurements: Spin echoes in the presence of a time-dependent field gradient. *J. Chem. Phys.* **1965**, *42*, 288–292. [[CrossRef](#)]
74. Skaanning, L.K.; Santoro, A.; Skamris, T.; Martinsen, J.H.; D’Ursi, A.M.; Bucciarelli, S.; Vestergaard, B.; Bugge, K.; Langkilde, A.E.; Kragelund, B.B. The non-fibrillating N-terminal of α -synuclein binds and co-fibrillates with heparin. *Biomolecules* **2020**, *10*, 1192. [[CrossRef](#)] [[PubMed](#)]
75. Schrödinger, L. *Maestro 12.5.139*; Schrödinger LLC: New York, NY, USA, 2018.

Disclaimer/Publisher’s Note: The statements, opinions and data contained in all publications are solely those of the individual author(s) and contributor(s) and not of MDPI and/or the editor(s). MDPI and/or the editor(s) disclaim responsibility for any injury to people or property resulting from any ideas, methods, instructions or products referred to in the content.